

Ferrocene-Containing Carbohydrate Dendrimers

Peter R. Ashton,^[d] Vincenzo Balzani,^[a] Miguel Clemente-León,^[a] Barbara Colonna,^[b] Alberto Credi,^{*,[a]} Narayanaswamy Jayaraman,^[c] Francisco M. Raymo,^{*,[b]} J. Fraser Stoddart,^[c] and Margherita Venturi^[a]

Abstract: Aliphatic amines, incorporating one or three (branched) acylated β -D-glucopyranosyl residues, were coupled with the acid chloride of ferrocenecarboxylic acid and with the diacid chloride of 1,1'-ferrocenedicarboxylic acid to afford four dendrimer-type, carbohydrate-coated ferrocene derivatives in good yields (54–92%). Deprotection of the peracylated β -D-glucopyranosyl residues was achieved quantitatively by using Zemplén conditions, affording four water-soluble ferrocene derivatives. When only one of the two cyclopentadienyl rings of the ferrocene unit is substituted, strong complexes are formed with β -cyclodextrin in H₂O, as demonstrated by liquid secondary ion mass spectrometry

(LSIMS), ¹H NMR spectroscopy, electrochemical measurements, and circular dichroism spectroscopy. Molecular dynamics calculations showed that the unsubstituted cyclopentadienyl ring is inserted through the cavity of the toroidal host in these complexes. The electrochemical behavior of the protected and deprotected ferrocene-containing dendrimers was investigated in acetonitrile and water, respectively. The diffusion coefficient decreases with in-

creasing molecular weight of the compound. The potential for oxidation of the ferrocene core, the rate constant of heterogeneous electron transfer, and the rate constant for the energy-transfer reaction with the luminescent excited state of the [Ru(bpy)₃]²⁺ complex (bpy = 2,2'-bipyridine) are strongly affected by the number (one or two) of substituents and by the number (one or three) of carbohydrate branches present in the substituents. These effects are assigned to shielding of the ferrocene core by the dendritic branches. Electrochemical evidence for the existence of different conformers for one of the dendrimers in aqueous solution was obtained.

Keywords: carbohydrates • cyclodextrins • dendrimers • electrochemistry • electron transfer • ferrocenes

Introduction

The reversible oxidation of ferrocene to the ferrocenium cation can be achieved chemically and/or electrochemically.^[1] In addition, synthetic approaches to ferrocene derivatives, bearing substituents on one or both cyclopentadienyl rings,

are well established.^[1] Thus, ferrocene is an ideal building block for the construction of both molecular and supramolecular systems,^[1] such as switches and sensors, which can be controlled by external stimuli.^[2] In view of these facts and given our interest in glycodendrimers construction,^[3] we were attracted by the possibility of attaching covalently carbohydrate residues to one or both of the cyclopentadienyl rings in ferrocene in order to confer water solubility and biocompatibility upon the metallocene. The steric bulk of the carbohydrate substituents can be increased by introducing one or more branching points, thus offering the opportunity of investigating the change in the redox behavior of the ferrocene core as a result of enlarging the surrounding carbohydrate shell. These water-soluble dendritic compounds,^[4, 5] containing redox-active cores,^[6] are reminiscent of the numerous naturally occurring water-soluble proteins^[7] with redox-active units embedded inside their polypeptidic frameworks. Furthermore, water-soluble ferrocene derivatives, in their neutral state, have been shown to be bound by β -cyclodextrin.^[8] Upon oxidation to the corresponding ferrocenium cation, the stability of the inclusion complex is expected to be impaired. As a result, the design of redox-active carbohydrate-based molecular-sized switches can be envis-

[a] Dr. A. Credi, Prof. V. Balzani, Dr. M. Clemente-León, Prof. M. Venturi
Dipartimento di Chimica "G. Ciamician"
Università degli Studi di Bologna
Via Selmi 2, 40126 Bologna (Italy)
Fax: (+39) 051-209-9456
E-mail: acredi@ciam.unibo.it

[b] Prof. F. M. Raymo, Dr. B. Colonna
Center for Supramolecular Science
Department of Chemistry, University of Miami
1301 Memorial Drive, Coral Gables, FL 33146-0431 (USA)
Fax: (+1) 305-284-4571
E-mail: fraymo@miami.edu

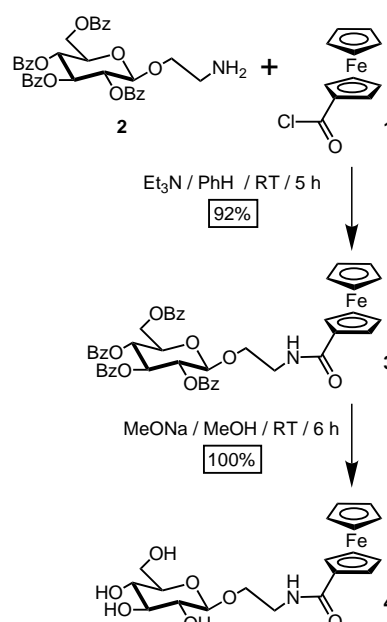
[c] Dr. N. Jayaraman, Prof. J. F. Stoddart
Department of Chemistry and Biochemistry
University of California, Los Angeles
405 Hilgard Avenue, Los Angeles, CA 90095-1569 (USA)

[d] P. R. Ashton
School of Chemistry, University of Birmingham
Edgbaston, Birmingham, B15 2TT (UK)

aged. Here, we report 1) the synthesis of four dendritic ferrocene derivatives incorporating fully protected β -D-glucopyranosyl residues on one or both cyclopentadienyl rings, 2) the production of their deprotected analogues, 3) the characterization of both the protected and deprotected species by mass spectrometry and NMR spectroscopy, 4) the complex formation between two of these carbohydrate-coated ferrocene derivatives and β -cyclodextrin, 5) a quantitative investigation of the electrochemical behavior (diffusion coefficients, redox potentials, heterogeneous electron-transfer rate constants) of the eight dendrimers, and 6) the rate constants of the energy-transfer reactions between the luminescent excited state of the $[\text{Ru}(\text{bpy})_3]^{2+}$ complex ($\text{bpy} = 2,2'$ -bipyridine) and these same compounds.

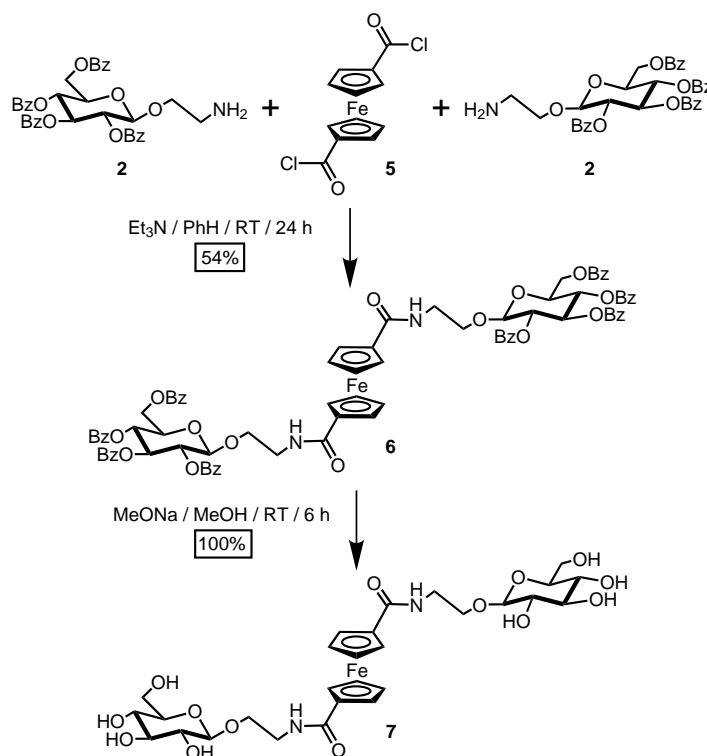
Results and Discussion

Synthesis and characterization: The protected dendrimers **3**, **6**, **9**, and **11** were obtained (Schemes 1–4) in good yields (54–92%) by reacting **1** or **5** with **2** or **8** in the presence of Et_3N . Removal of the protecting groups of **3**, **6**, **9**, and **11** with



Scheme 1. Synthesis of the monosubstituted ferrocene derivatives **3** and **4**.

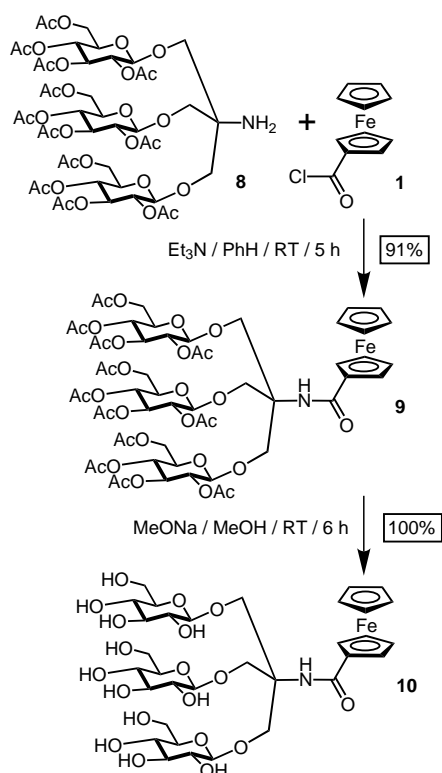
Abstract in Italian: Condensando ammine alifatiche, contenenti uno o tre residui β -D-glucopiranosilici protetti, con il cloruro dell'acido ferrocenecarbossilico o dell'acido 1,1'-ferrocenedicarbossilico, sono stati ottenuti con buone rese (54–92%) quattro composti di tipo dendritico caratterizzati dal fatto di avere il ferrocene come unità centrale ed un guscio esterno costituito da carboidrati. Mediante deprotezione quantitativa dei residui β -D-glucopiranosilici perbenzoilati o peracetilati, ottenuta in condizioni di Zémpfen, sono stati preparati quattro derivati dendritici del ferrocene solubili in acqua. I composti in cui solo uno dei due anelli ciclopentadienilici del ferrocene è sostituito formano, in H_2O , complessi stabili con la β -ciclodestrina, come dimostrato da esperimenti di spettrometria di massa LSIMS e di spettroscopia ^1H NMR, da misure elettrochimiche e da spettri di dicroismo circolare. Calcoli di dinamica molecolare hanno evidenziato che, in questi complessi, l'anello ciclopentadienilico non sostituito è inserito nella cavità toroidale della β -ciclodestrina. Lo studio elettrochimico dei dendrimeri protetti e deprotetti è stato effettuato rispettivamente in acetonitrile e in acqua. Il coefficiente di diffusione decresce all'aumentare della massa molecolare del composto; il numero di sostituenti (uno o due) e delle ramificazioni (una o tre) presenti nei sostituenti stessi influenza fortemente il potenziale al quale avviene l'ossidazione dell'unità centrale di ferrocene, la costante di velocità del trasferimento elettronico eterogeneo e la costante di velocità del processo di trasferimento di energia con lo stato eccitato luminescente del complesso metallico $[\text{Ru}(\text{bpy})_3]^{2+}$ ($\text{bpy} = 2,2'$ -dipiridina). Questi effetti sono attribuiti alla schermatura esercitata dalle ramificazioni dendritiche sull'unità centrale di ferrocene. Nel caso di uno dei dendrimeri studiati, gli esperimenti elettrochimici hanno anche evidenziato l'esistenza, in soluzione acquosa, di due diversi conformeri.



Scheme 2. Synthesis of the disubstituted ferrocene derivatives **6** and **7**.

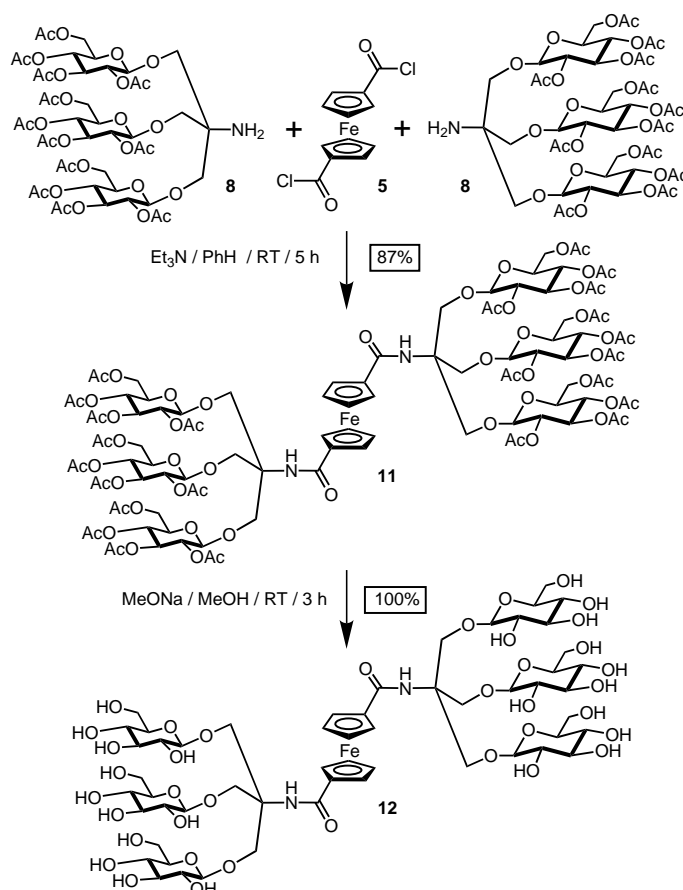
NaOMe in MeOH quantitatively afforded **4**, **7**, **10**, and **12**, respectively.

All compounds were characterized by low- and high-resolution liquid secondary-ion mass spectrometry (LSIMS), as well as by ^1H and ^{13}C NMR spectroscopy. The LSIMS revealed peaks corresponding to either $[M]^+$ or $[M+H]^+$ ions (Table 1). The signals in the ^1H NMR spectra of the protected species **3**, **6**, **9**, and **11** (Table 2), as well as of the deprotected species **4**, **7**, **10**, and **12** (Table 3), were assigned unambigu-



Scheme 3. Synthesis of the monosubstituted ferrocene derivatives **9** and **10**.

ously by two-dimensional homonuclear and heteronuclear correlation NMR spectroscopy. In the ^1H NMR spectra (CDCl_3 , 25°C) of **3** and **9**, the protons on the unsubstituted cyclopentadienyl ring resonate as a singlet at approximately $\delta = 4.2$. In both instances, three additional sets of signals are observed at about $\delta = 4.3$, 4.5 , and 4.6 for the protons of the substituted cyclopentadienyl ring. The ^1H NMR spectrum (CDCl_3 , 25°C) of **6** reveals only two singlets at $\delta = 4.20$ and 4.44 for the cyclopentadienyl protons. By contrast, four broad singlets are observed at $\delta = 4.40$, 4.51 , 4.67 , and 4.71 for the cyclopentadienyl protons in the case of **11**. The ^1H NMR spectra (D_2O , 25°C) of **4** and **10** show a singlet at approximately $\delta = 4.2$ for the protons of the unsubstituted cyclo-

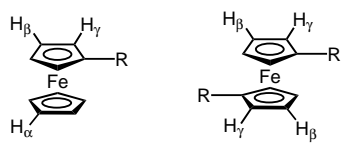


Scheme 4. Synthesis of the disubstituted ferrocene derivatives **11** and **12**.

Table 1. Liquid secondary-ion mass spectrometric (LSIMS) data of the compounds **3**, **4**, **6**, **7**, and **9–12**.

	Molecular formula	Observed ion
3	$\text{C}_{47}\text{H}_{41}\text{FeNO}_{11}$	851 $[M]^+$
4	$\text{C}_{19}\text{H}_{25}\text{FeNO}_7$	436 $[M+H]^+$
6	$\text{C}_{84}\text{H}_{72}\text{FeN}_2\text{O}_{22}$	1518 $[M+H]^+$
7	$\text{C}_{28}\text{H}_{40}\text{FeN}_2\text{O}_{14}$	685 $[M+H]^+$
9	$\text{C}_{57}\text{H}_{73}\text{FeNO}_{31}$	1323 $[M]^+$
10	$\text{C}_{33}\text{H}_{50}\text{FeNO}_{19}$	820 $[M+H]^+$
11	$\text{C}_{104}\text{H}_{136}\text{FeN}_2\text{O}_{62}$	2462 $[M+H]^+$
12	$\text{C}_{56}\text{H}_{88}\text{FeN}_2\text{O}_{38}$	1453 $[M+H]^+$

Table 2. ^1H NMR spectroscopic data (δ values in ppm) of the protected compounds **3**, **6**, **9**, and **11** in CDCl_3 at 25°C .^[a]

								Cyclopentadienyl protons			
	H-1	H-2	H-3	H-4	H-5	H-6 a	H-6 b	H _α	H _β and H _γ		
3	4.95 (d, 1H)	5.62 (dd, 1H)	5.99 (pt, 1H)	5.75 (pt, 1H)	4.21–4.25 (m, 1H)	4.55 (dd, 1H)	4.70 (dd, 1H)	4.17 (s, 5H)	4.21–4.25 (m, 2H)	4.50 (brs, 1H)	4.61 (brs, 1H)
6	5.62 (d, 2H)	5.65 (dd, 2H)	5.78 (pt, 2H)	6.01 (pt, 2H)	4.22–4.28 (m, 2H)	4.55 (dd, 2H)	4.71 (dd, 2H)		4.20 (s, 4H)	4.44 (s, 4H)	
9	4.47 (d, 3H)	4.97 (dd, 3H)	5.17 (pt, 3H)	5.04 (pt, 3H)	3.61–3.71 (m, 3H)	4.23–4.32 (m, 3H)	4.09 (dd, 3H)	4.21 (s, 5H)	4.23–4.32 (m, 2H)	4.51 (brs, 1H)	4.68 (brs, 1H)
11	4.55 (d, 6H)	5.02 (dd, 6H)	5.24 (pt, 6H)	5.10 (pt, 6H)	3.74–3.79 (m, 6H)	4.36 (dd, 6H)	4.15 (dd, 6H)	4.40 (brs, 2H)	4.51 (brs, 2H)	4.67 (brs, 2H)	4.71 (brs, 2H)

[a] The signals were assigned by two-dimensional homonuclear and heteronuclear correlation NMR spectroscopy.

Table 3. ^1H NMR spectroscopic data (δ values in ppm) of the deprotected compounds **4**, **7**, **10**, and **12** in D_2O at 25°C .^[a]

	β -D-Glucopyranosyl protons						Cyclopentadienyl protons			
	H-1	H-2	H-3	H-4	H-5	H-6a	H-6b	H _{α}	H _{β} and H _{γ}	
4	4.41 (d, 1H)	3.23 (dd, 1H)	3.41 (pt, 1H)	3.28 (pt, 1H)	3.34–3.38 (m, 1H)	3.62 (dd, 1H)	3.82 (dd, 1H)	4.21 (s, 5H)	4.44 (brs, 2H)	4.72 (brs, 2H)
7	4.41 (d, 2H)	3.16–3.29 (m, 2H)	3.32–3.42 (m, 2H)	3.16–3.29 (m, 2H)	3.32–3.42 (m, 2H)	3.56–3.64 (m, 2H)	3.77–3.84 (m, 2H)		4.45 (brs, 2H)	4.66 (brs, 2H)
10	4.31 (d, 3H)	3.13 (dd, 3H)	3.30 (pt, 3H)	3.16 (pt, 3H)	3.23–3.27 (m, 3H)	3.52 (dd, 3H)	3.71 (dd, 3H)	4.15 (s, 5H)	4.34 (brs, 2H)	4.63 (brs, 2H)
12	4.40 (d, 6H)	3.22 (dd, 6H)	3.39 (pt, 6H)	3.26 (pt, 6H)	3.31–3.37 (m, 6H)	3.60 (dd, 6H)	3.80 (dd, 6H)		4.50 (brs, 4H)	4.80 (brs, 4H)

[a] The signals were assigned by two-dimensional homonuclear and heteronuclear correlation NMR spectroscopy.

pentadienyl ring and two broad singlets ($\delta = 4.44$ and 4.72 for **4**, $\delta = 4.34$ and 4.63 for **10**) for the protons on the substituted cyclopentadienyl ring. In the case of **7**, the cyclopentadienyl protons give rise to four sets of signals at $\delta = 4.45$, 4.66 , 4.81 , and 4.87 . By contrast, only two sets at $\delta = 4.50$ and 4.80 are observed for the cyclopentadienyl protons of **12**.

In order to visualize the preferred conformations of the protected and deprotected mono- and disubstituted ferrocene derivatives, their global minima were probed for by molecular dynamics calculations. The global minima found for the protected dendrimers **3**, **6**, **9**, and **11**, as well as those found for the deprotected ones **4**, **7**, **10**, and **12**, are illustrated in Figures 1 and 2, respectively. In the monosubstituted derivatives **3**, **4**, **9**, and **10**, the substituent “wraps” itself around the unsubstituted cyclopentadienyl ring as a result of C–H \cdots O contacts between the cyclopentadienyl protons and the oxygen atoms of β -D-glucopyranosyl residues. In addition, the phenyl ring of the benzoyl group in the 6-position of the

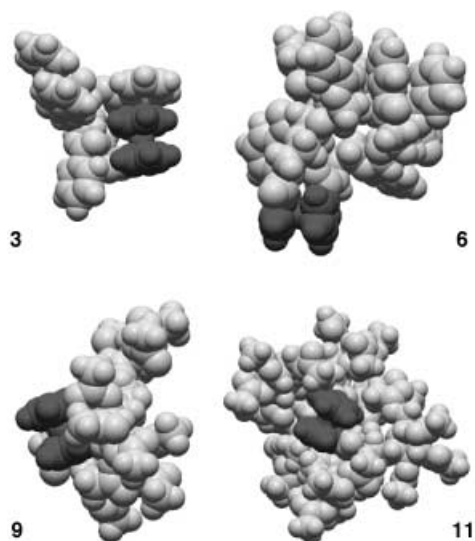


Figure 1. Space-filling representation of the conformational global minima of the protected compounds **3**, **6**, **9**, and **11** found by molecular dynamics calculations, followed by multiconformer minimizations.

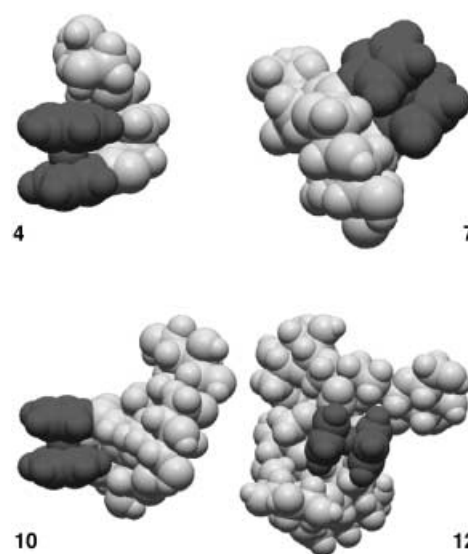


Figure 2. Space-filling representation of the conformational global minima of the deprotected compounds **4**, **7**, **10**, and **12** found by molecular dynamics calculations, followed by multiconformer minimizations.

perbenzoylated β -D-glucopyranosyl residue of **3** stacks alongside its unsubstituted cyclopentadienyl ring. In the disubstituted species **6**, **7**, **11**, and **12**, the two bulky substituents do not point away from each other. Rather, they are “glued” together by hydrogen-bonding interactions 1) between the amide groups and 2) between the deprotected β -D-glucopyranosyl residues. It is interesting to note the size of the carbohydrate shell relative to the ferrocene core, which, in the case of the largest dendrimer **11**, is embedded completely into the surrounding carbohydrate framework.

All the carbohydrate-coated ferrocene derivatives—protected species in MeCN and deprotected ones in H_2O —exhibit the same absorption spectrum in the visible region, consisting of a broad and weak band ($\lambda_{\text{max}} = 440 \text{ nm}$; $\epsilon \approx 300 \text{ L mol}^{-1} \text{ cm}^{-1}$). Comparison with the absorption spectrum of ferrocene in acetonitrile shows that this band is caused by the d–d transition of the ferrocene moiety.^[9] Below 380 nm ,

the intensity of the absorption spectrum rises with the increasing number of branches. Ferrocene does not exhibit luminescence^[10] and, as expected, nor does any of its derivatives.

Electrochemical behavior: The eight carbohydrate-coated ferrocene derivatives with their dendritic structures can be divided into two families—namely, protected (**3**, **6**, **9**, **11**) and deprotected (**4**, **7**, **10**, **12**) species. The protected dendrimers are soluble in organic solvents and have been studied in MeCN, whereas the deprotected ones are soluble in H₂O and so have been studied in this solvent. Both families consist of four compounds, namely mono- and disubstituted species obtained by using singly- and triply-branched substituents. It should be noted that the family of the protected dendrimers is less homogeneous constitutionally than that of the deprotected ones because the protecting groups are different for the singly- and triply-branched species.

In the potential window examined (−2/+2 V vs SCE in MeCN for the protected compounds, −1/+1 V vs SCE in H₂O for the deprotected ones), all the dendrimers show the characteristic oxidation process of the ferrocene moiety and no reduction process. In discussing the electrochemical behavior of these species, it is appropriate to consider CPK space-filling molecular models or the illustrations (Figures 1 and 2) based on molecular dynamics calculations which reveal clearly the shapes and relative dimensions of the subunits in each dendrimer.

Protected derivatives 3, 6, 9, and 11: The values of the halfwave potential for the oxidation of the ferrocene core, the diffusion coefficient, the electron-transfer coefficient, and heterogeneous electron-transfer rate constant are shown in Table 4. Note that, as expected, the values of the diffusion

Table 4. Electrochemical data for the protected dendrimers (MeCN, 0.05 mol L^{−1} TBAPF₆, 22 °C, glassy carbon electrode).

	MW [g mol ^{−1}]	$E_{1/2}$ [V vs SCE]	$D_0 \times 10^6$ [cm ² s ^{−1}]	α	k_0 [cm s ^{−1}]
3	849.7	0.560 ± 0.003	6.9 ± 0.7	0.5	0.08 ± 0.03
6	1515.3	0.730 ± 0.003	4.7 ± 0.5	0.4	0.03 ± 0.01
9	1322.0	0.580 ± 0.003	5.5 ± 0.6	0.4	0.015 ± 0.005
11	2460.0	0.779 ± 0.003	2.4 ± 0.3	0.4	0.003 ± 0.001

coefficients decrease with increasing molecular weights. In addition, the electrochemical data point to some interesting trends which include the following: 1) The potential for the oxidation of the ferrocene core increases on going from the monosubstituted compounds to disubstituted ones—an observation which can be ascribed to the slightly electron-acceptor character of the amidic substituents as well as to the shielding of the ferrocene core by the appended substituents, so that the ferrocenium ion resulting from the oxidation process is considerably less stabilized by interactions with the polar solvent molecules. 2) For both the mono- and disubstituted species, the potential value becomes more positive with increasing branching of the substituent; furthermore, the effect is larger for the disubstituted compounds. These effects can be accounted for by the fact that the ferrocene core becomes more and more shielded from solvent interactions on

increasing the number and size of the appended moieties. The effects are smaller for the monosubstituted derivatives because one side of the ferrocene core remains open to solvent interactions. We will see, subsequently, that these results are fully consistent with the values obtained for the heterogeneous electron-transfer rate constants. 3) For both the mono- and disubstituted compounds, the rate constants for the heterogeneous electron-transfer processes are observed to decrease on increasing branching of the substituent; once again, the effect is larger for the disubstituted species, for which the rate constants are observed to decrease by a factor of ten. It should also be noted that the value of the rate constant for the monosubstituted triply-branched dendrimer **9** is smaller than that for the heavier and larger disubstituted singly-branched derivative **6**, suggesting that a triply-branched substituent is more effective at isolating the electroactive core than two singly branched substituents, which, as indicated by molecular modeling (Figure 1), are located on the same side of the ferrocene core.

Deprotected derivatives 4, 7, 10, and 12: The values, obtained in aqueous solution, of the halfwave potential for the oxidation of the ferrocene core, the diffusion coefficient, the electron-transfer coefficient, and the heterogeneous electron-transfer rate constant of **4**, **7**, **10**, and **12** are shown in Table 5. This family is considered to be homogeneous, since all the deprotected carbohydrate units are identical. Although the values of the diffusion coefficient decrease with increasing molecular weights, they are smaller than those for the protected derivatives (Table 4), in spite of the fact that the deprotected ones are much lighter. This result can be accounted for by 1) the difference in the macroscopic viscosity of the two solvents^[11] and 2) different friction effects at the molecular level.^[12]

Table 5. Electrochemical data for the deprotected dendrimers (H₂O, 0.1 mol L^{−1} NaClO₄, 22 °C, glassy carbon electrode).

	MW [g mol ^{−1}]	$E_{1/2}$ [V vs SCE]	$D_0 \times 10^6$ [cm ² s ^{−1}]	α	k_0 [cm s ^{−1}]
4	433.2	0.373 ± 0.005	3.0 ± 0.4	0.5	0.028 ± 0.005
7	682.5	0.605 ± 0.005	2.3 ± 0.4	0.6	0.009 ± 0.002
10	817.5	0.413 ± 0.004	1.9 ± 0.4	0.4	0.013 ± 0.004
12	1451.5	0.54 ± 0.01 ^[a] 0.64 ± 0.01 ^[a]	1.5 ± 0.2	^[b]	^[b]

[a] Overlapping processes; potential values estimated from the deconvolution of the DPV profile. See text for details. [b] The values of α and k_0 for compound **12** could not be estimated reliably.

In general, the values (Table 5) of the halfwave potential for the oxidation of the ferrocene core are less positive than those observed for the protected dendrimers (Table 4). This result can be attributed to the greater stabilization of the ferrocenium species in the more polar aqueous medium. As in the case of the protected derivatives, the value of the redox potential becomes more positive 1) in going from the mono- to the disubstituted species, because of the greater number of electron-withdrawing amide-type substituents, and 2) on increasing branching, for both the mono- and disubstituted compounds, owing to the shielding provided by the carbohydrate units toward the ferrocene core interacting with the

solvent. The latter effect is stronger than that observed for the protected derivatives in MeCN solution, at least for the monosubstituted species; the increase in the potential value is 40 mV (Table 5) on going from the singly-branched deprotected dendrimer **4** to the triply-branched dendrimer **10**, while it is only 20 mV (Table 4) on going from the corresponding protected species **3** to **9**. This observation is in agreement with the larger difference in polarity between the environment offered to the electroactive core by the glucopyranosyl branches and that of the two different solvents (H₂O and MeCN).

The triply-branched disubstituted derivative **12** exhibits a very peculiar behavior. Its differential pulse voltammogram reveals two oxidation peaks—the first one at +0.54 V and the second one at +0.64 V—with an intensity ratio of approximately 1:2 (Figure 3). This behavior suggests that, in aqueous solution, derivative **12** is present in two distinguishable forms

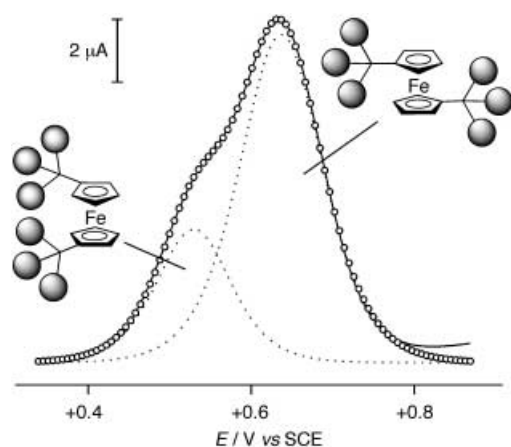


Figure 3. Differential pulse voltammogram of compound **12** ($1 \times 10^{-3} \text{ mol L}^{-1}$, H₂O, $0.1 \text{ mol L}^{-1} \text{ NaClO}_4$, 22°C ; glassy carbon electrode, scan rate 20 mV s^{-1} , pulse height 75 mV). The potential values have been corrected for the pulse height. The circles show a simulated DPV profile consisting of the sum of two individual peaks of different intensities (dotted lines). For more details, see text.

that experience different shielding effects at this electroactive ferrocene cores. The reversible character of the two oxidation processes shows that the interconversion between these two species is slow on the timescale of the electrochemical experiments. The simplest hypothesis that accounts for the observed results is the existence of two conformers of **12** (Figure 3), one having the two substituents placed on the same (*cisoid*) side of the ferrocene core and the other on opposite (*transoid*) sides. The *cisoid* form, which can be stabilized by intramolecular hydrogen bonds, will be less shielded from solvent interactions than the *transoid* form and will therefore be easier to oxidize. If this hypothesis is correct, the processes observed at +0.54 and +0.64 V correspond to the oxidation of the *cisoid* and *transoid* conformers of **12**, respectively. In the light of this conclusion, the high value of the potential exhibited by **7** indicates a *transoid* conformation predominantly for this compound in aqueous solution.^[13]

The magnitudes of the heterogeneous electron-transfer rate constants (Table 5) are consistent with the above conclusions.

In particular, the fact that the value found for the disubstituted singly-branched species **7** is smaller than that found for the monosubstituted triply-branched derivative **10**—contrary to what happens for the analogous protected compounds **6** and **9**—is consistent with a *transoid* configuration for **7**. The rate constants are much smaller for the deprotected mono- and disubstituted singly-branched derivatives **4** and **7** relative to those for the corresponding protected species **3** and **6**. This effect arises, partly at least, from the higher reorganization energy of the oxidation process in H₂O than in MeCN.

Quenching of the $[\text{Ru}(\text{bpy})_3]^{2+}$ luminescence: It is well known that excitation of $[\text{Ru}(\text{bpy})_3]^{2+}$ (bpy = 2,2'-bipyridine) with visible light leads to the formation of a metal-to-ligand charge-transfer (MLCT) singlet excited state which then undergoes deactivation to the lowest MLCT triplet,^[14] hereafter indicated by $^*[\text{Ru}(\text{bpy})_3]^{2+}$. Such an excited state shows a long-lived luminescence ($\tau = 172 \text{ ns}$ in aerated MeCN solution at 298 K), which lies 2.12 eV above the ground state, and can play the role of an oxidant ($E_{1/2}\{^*[\text{Ru}(\text{bpy})_3]^{2+}/[\text{Ru}(\text{bpy})_3]^{2+}\} = +0.80 \text{ V vs SCE in MeCN}$).

We have investigated the quenching of the $^*[\text{Ru}(\text{bpy})_3]^{2+}$ luminescent excited state by 1) ferrocene and the protected derivatives **3**, **6** and **9** (**11** was not available in a sufficient amount) in MeCN containing $0.05 \text{ mol L}^{-1} \text{ TBAPF}_6$, and 2) the ferrocenecarboxylate anion and the deprotected species **4**, **10**, and **12** (**7** was not available in a sufficient amount) in H₂O containing $0.05 \text{ mol L}^{-1} \text{ NaClO}_4$. The solutions were air-equilibrated, and both intensity and lifetime quenching measurements were performed. In all cases, the quenching of the intensity was larger than that of the lifetime, suggesting the presence of some associated $[\text{Ru}(\text{bpy})_3]^{2+}$ –dendrimer species in which static quenching takes place.^[15]

Dynamic quenching takes place through diffusion-controlled formation of encounter complexes between the excited state and the quencher, followed by some quenching interaction between the two reaction partners. The values of the dynamic quenching constant, obtained from Stern–Volmer plots based on lifetime measurements (Table 6), are all below the diffusion rate constants k_d of the solvent used ($1.9 \times 10^{10} \text{ L mol}^{-1} \text{ s}^{-1}$ in MeCN and $7.4 \times 10^9 \text{ L mol}^{-1} \text{ s}^{-1}$ in H₂O at 298 K).^[16] This observation means that the rate-limiting step of the quenching process is that within the encounter complex

Table 6. Experimental (k_q) and diffusion-corrected (k_{cor}) quenching rate constants of $[\text{Ru}(\text{bpy})_3]^{2+}$ by ferrocene, protected dendrimers **3**, **6**, and **9**, ferrocenecarboxylate anion, and deprotected dendrimers **4**, **10**, and **12**.

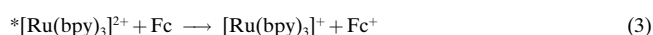
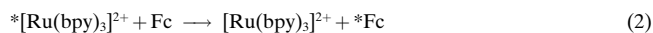
Quencher	Solvent	$k_q \times 10^{-9}$ [L mol ⁻¹ s ⁻¹]	$k_{\text{cor}} \times 10^{-9}$ [L mol ⁻¹ s ⁻¹] ^[a]
Fc	MeCN, TBAPF ₆ (0.05 mol L^{-1})	7.8 ± 0.8	13 ± 1
3	MeCN, TBAPF ₆ (0.05 mol L^{-1})	3.3 ± 0.3	4.0 ± 0.4
6	MeCN, TBAPF ₆ (0.05 mol L^{-1})	1.6 ± 0.2	1.7 ± 0.2
9	MeCN, TBAPF ₆ (0.05 mol L^{-1})	1.9 ± 0.4	2.1 ± 0.4
Fc-COO ⁻	H ₂ O, NaClO ₄ (0.05 mol L^{-1})	3.5 ± 0.4	6.6 ± 0.8
4	H ₂ O, NaClO ₄ (0.05 mol L^{-1})	2.1 ± 0.2	2.9 ± 0.3
10	H ₂ O, NaClO ₄ (0.05 mol L^{-1})	1.4 ± 0.2	1.7 ± 0.2
12	H ₂ O, NaClO ₄ (0.05 mol L^{-1})	1.2 ± 0.2	1.4 ± 0.2

[a] Quenching rate constant corrected for diffusional effects; see text for details.

for which the rate constant is proportional to k_{cor} as obtained^[17] from Equation (1):

$$1/k_{\text{cor}} = 1/k_q - 1/k_d \quad (1)$$

The values of k_{cor} are also listed in Table 6. In the case of ferrocene, the lowest excited state lies less than 1.8 eV above its ground state^[18, 19] and the Fc^+/Fc reduction potential is +0.40 V versus SCE. Therefore, if we consider the excited state energy and the reduction potential of the luminescent excited state of $[\text{Ru}(\text{bpy})_3]^{2+}$ (vide supra), both the energy-transfer [Eq. (2)] and electron-transfer [Eq. (3)] quenching processes turn out to be thermodynamically allowed:



Lee and Wrighton,^[19] however, have shown that, in the case of ferrocene, quenching takes place only by energy transfer, presumably because the electron-transfer process is slowed down by the large reorganizational energy required by ferrocene oxidation in polar solvents. For methyl derivatives of ferrocene, which are much easier to oxidize, competitive energy- and electron-transfer quenching has been observed.^[19] Since oxidation of the ferrocene core of the protected dendrimers takes place at potential values more positive than that of ferrocene, it seems safe to assume that the quenching processes studied in MeCN solutions take place only by energy transfer. This conclusion can probably be extended to the processes involving the deprotected derivatives, because of the larger reorganizational energy required by the electron-transfer quenching in the more polar aqueous solution.

Energy-transfer quenching can occur by two different mechanisms. One may be viewed as a resonance dipole–dipole effect (Förster mechanism),^[20] and the other as a double electron exchange (Dexter mechanism).^[21] As recently pointed out by Encinas et al.,^[22] the overlap integral between the $[\text{Ru}(\text{bpy})_3]^{2+}$ -type luminescence and the ferrocene-type absorption bands is so small that energy transfer by the Förster mechanism can be ruled out. The only plausible quenching mechanism is therefore the Dexter one, whose rate constant can be expressed^[23] by Equation (4):

$$k_{\text{en}} = (4\pi^2/h) H^2 J_D \quad (4)$$

in which H is the matrix element for electronic coupling between donor and acceptor and J_D is the Franck–Condon term, which is related to overlap integrals between the luminescence spectrum of the donor and the absorption spectrum of the acceptor. Since the absorption spectrum of the ferrocene acceptor moiety is essentially the same for all the examined compounds, the J_D term should be constant, and the decrease of k_{cor} (which is proportional to k_{en}) on increasing number of substituents (**3** vs **6**, **10** vs **12**) and number of branches (**3** vs **9**, **4** vs **10**) must arise from different electronic interaction values. This conclusion fully agrees with the expected shielding effects on the ferrocene core by substituents and branches.

Binding studies: The monosubstituted ferrocene derivatives **4** and **10** are bound by β -cyclodextrin (β -CD) in D_2O (Figure 4). The LSIMS of equimolar mixtures of β -CD and either **4** or **10** revealed peaks at m/z 1570 or 1954, respectively, for the

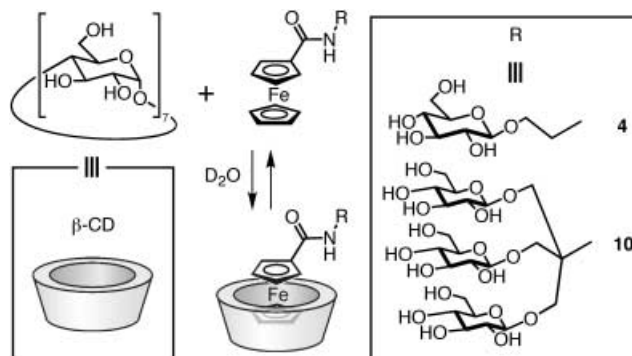


Figure 4. The complexation of the monosubstituted ferrocene derivatives **4** and **10** by β -cyclodextrin (β -CD).

corresponding 1:1 complexes. In D_2O at 25 °C, the complexation/decomplexation processes are slow on the ^1H NMR timescale (500 MHz). As a result, the sharp and well-resolved signals for protons in the uncomplexed species (Figure 5a) become broad and unresolved in the presence of β -CD

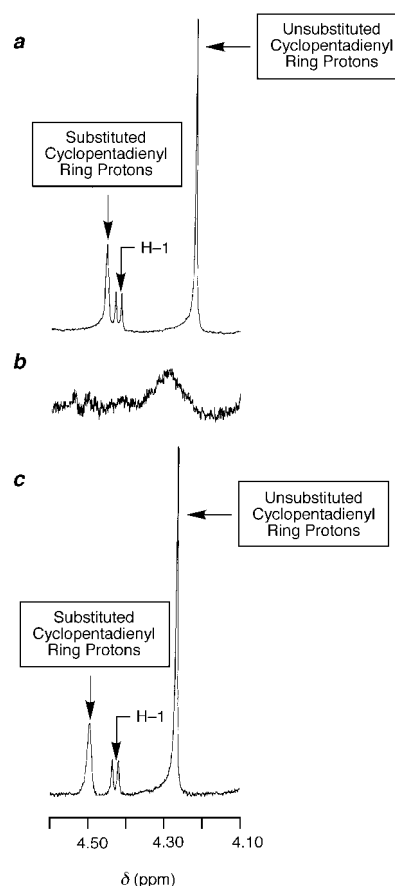


Figure 5. Partial ^1H NMR spectra (500 MHz, D_2O , 25 °C) of a) **4**, b) a 4:1 mixture of β -cyclodextrin (β -CD) and **4**, and c) a 10:1 mixture of β -CD and **4**.

(Figure 5b). After the addition of more than seven equivalents of β -CD, most of the guest present in solution is bound by β -CD, and sharp and well-resolved resonances are observed once again. However, while the chemical shifts of the resonances associated with the β -D-glucopyranosyl protons of **4** and **10** are almost unchanged on complexation (compare the signals associated with H-1 in Figure 5a and 5c), the resonances of the cyclopentadienyl protons shift upfield. Interestingly, when the disubstituted ferrocene derivatives **7** and **11** are mixed with β -CD under the same conditions, no significant changes in their ^1H NMR spectra occur. In support of this observation, peaks for complexed species are *not* observed by LSIMS, suggesting that these compounds are *not* bound by β -CD. Molecular dynamics calculations performed on the complexes, revealed (Figure 6) that the unsubstituted cyclopentadienyl rings of **4** and **10** are located inside the cavity of β -CD, while the substituted cyclopentadienyl rings, with the attached carbohydrate residues, protrude outside.^[24] In **7** and **11**, both cyclopentadienyl rings bear bulky substituents and, as a result, cannot fit inside the cavity of β -CD.

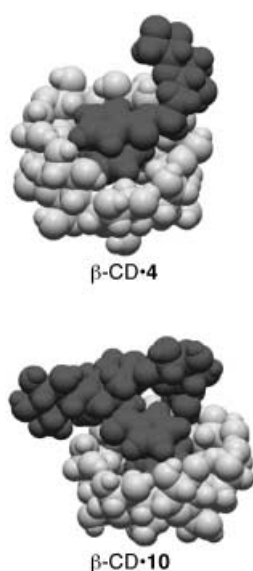


Figure 6. Space-filling representation of the global minima of the complexes formed between the monosubstituted ferrocene derivatives **4** and **10** and β -cyclodextrin (β -CD) found by molecular dynamics calculations followed by multiconformer minimizations.

We have investigated the effect of the addition of β -CD on the electrochemical behavior of the deprotected derivatives **4**, **7**, **10**, and **12** in aqueous solution. Clear changes in the voltammetric behavior were observed for the monosubstituted compounds **4** (Figure 7) and **10**, whereas no effect was found in the case of the disubstituted species **7** and **12**, even after addition of β -CD up to a concentration close to that of the saturation value (ca. $10^{-2} \text{ mol L}^{-1}$). These results confirm that—as shown by NMR measurements—only the monosubstituted derivatives associate with β -CD. For **4** and **10**, we have found that, on addition of β -CD, the oxidation wave remains reversible, but moves toward more positive values and decreases in intensity. These effects can be attributed to the stabilization of the neutral ferrocene moiety on inclusion

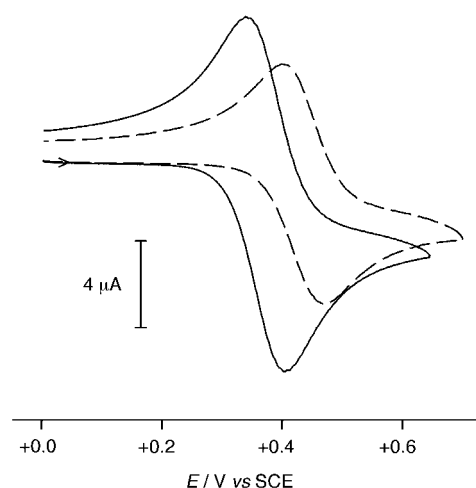


Figure 7. Cyclic voltammetric behavior of compound **4** in the absence (full line) and in the presence (dashed line) of 10 equiv of β -CD. Conditions: $1 \times 10^{-3} \text{ mol L}^{-1}$, H_2O , $0.1 \text{ mol L}^{-1} \text{ NaClO}_4$, 22°C ; glassy carbon electrode, scan rate 100 mV s^{-1} .

inside the β -CD cavity and to the decrease in the diffusion coefficient of the $[\mathbf{4} \cdot \beta\text{-CD}]$ and $[\mathbf{10} \cdot \beta\text{-CD}]$ adducts, relative to the free **4** and **10** species.

The chemical–electrochemical mechanism previously discussed by Evans, et al.^[8g] and, later, by Kaifer, et al.^[8m] for the electrochemical behavior of ferrocene in the presence of β -CD [Eqs. (5) and (6)] can be used to explain the results obtained:



In other words, only the uncomplexed ferrocene species are electroactive, and, therefore, the electron-transfer process must be preceded by decomplexation. The diffusion coefficient of the adduct can be obtained^[8g] from the ratio of the current peak values observed in the absence and in the presence of an excess of β -CD, and the stability constant can be calculated from simulations of the voltammetric curves obtained at different β -CD concentrations. The values of the diffusion coefficients and stability constants are shown in Table 7. It should be noted that the stability constants are of the same order of magnitude as that observed for the ferrocenecarboxylate anion and β -CD ($K_{\text{stab}} = 2200 \text{ L mol}^{-1}$) by Evans et al.^[8g] and larger than those found by Kaifer et al.^[5m] for ferrocene with appended polyamide branches. The decrease in the association constant on going from **4** to **10** is not surprising in view of the larger size of the substituent in the latter compound.

Table 7. Stability constants and diffusion coefficients of the complexes formed between β -CD and dendrimers **4** and **10** (H_2O , $0.1 \text{ mol L}^{-1} \text{ NaClO}_4$, 22°C).

	$K_{\text{stab}} [\text{L mol}^{-1}]$	$D_{\text{C}} \times 10^6 [\text{cm}^2 \text{s}^{-1}]$
4	2000 ± 200	1.3 ± 0.2
10	1300 ± 200	1.0 ± 0.2

Since it is known that inclusion of achiral guests into the chiral cavity of β -CD induces circular dichroism in the absorption bands of the guest,^[25] we have investigated the association of the deprotected derivatives with β -CD by circular dichroism spectroscopy. It should be noted that, in the compounds under investigation here, the achiral ferrocene core is linked to chiral carbohydrate residues. For this reason, **4** and, particularly, **10** (Figure 8, curve a) already exhibit a

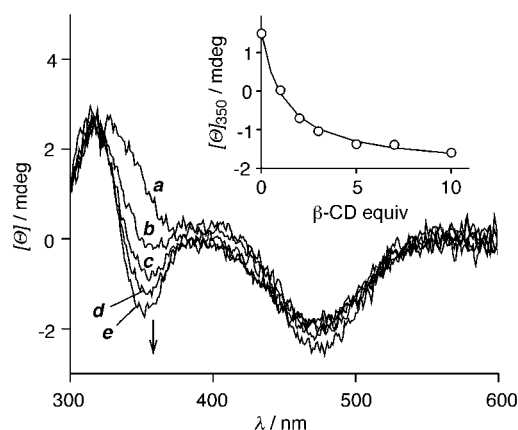


Figure 8. Circular dichroism spectral changes ($1 \times 10^{-3} \text{ mol L}^{-1}$, H_2O , 22°C) of compound **10** in the absence (a) and in the presence of increasing amounts of β -CD (b: 1 equiv; c: 2 equiv; d: 3 equiv; e: 10 equiv). The inset shows a titration curve based on the circular dichroism changes at 350 nm.

circular dichroism signal in the region of the ferrocene bands. Since the through-bond electronic interaction of the carbohydrate moieties with the (remote) ferrocene unit is likely to be very small, it seems more probable that the induced circular dichroism is caused by through-space interactions, which are expected to be qualitatively different and quantitatively stronger in the case of the triply-branched substituent of **10**. On addition of β -CD to aqueous solutions of **4** and **10**, small changes are observed in the circular dichroism (see, e.g., Figure 8). In the case of **10**, from a titration curve based on the value of the signal at 350 nm (Figure 8, inset), an association constant of approximately 10^3 L mol^{-1} was obtained, in fair agreement with the value obtained from voltammetric measurements (vide infra).

Conclusion

The covalent attachment of carbohydrate shells to ferrocene cores has been realized by amide-bond formation. The carbohydrate framework affects greatly the properties of the core by conferring upon it water solubility and by influencing its redox behavior. When only one β -D-glucopyranosyl-containing substituent is attached to a ferrocene core, the hydrophobic redox active unit is bound by β -cyclodextrin in H_2O , leading to complexes composed of a carbohydrate-based host and a carbohydrate-containing guest. In these complexes, the unsubstituted cyclopentadienyl ring of the ferrocene unit is located inside the cavity of the host. By contrast, when β -D-glucopyranosyl-containing substituents are attached to both

the cyclopentadienyl rings on the ferrocene core, no complexation occurs.

A quantitative investigation has been performed on the electrochemical behavior (diffusion coefficients, redox potentials, rates of heterogeneous electron transfer) of the eight dendritic compounds and on the rates of the energy-transfer quenching process of the luminescent excited state of the $[\text{Ru}(\text{bpy})_3]^{2+}$ complex by the dendrimers. The results obtained have shown that the number (one or two) of substituents and the number (one or three) of carbohydrate branches present in the substituents play a crucial role in protecting the ferrocene core from solvent interactions, as well as from interactions with an electrode or a partner in an encounter complex. The examined species mimic the behavior of proteins incorporating a redox active unit embedded into a polypeptidic framework. For the monosubstituted derivatives soluble in aqueous solution, the effect of inclusion of the ferrocene moiety in the cavity of β -cyclodextrin has also been investigated with a variety of techniques. Electrochemical evidence for the existence of different conformers for one of the dendrimers in aqueous solution has been obtained, opening the way to processes capable of mimicking effects related to the tertiary structure of proteins.

Experimental Section

General methods: Chemicals were purchased from Aldrich and used as received. Solvents were dried according to literature procedures.^[26] The compounds **1**,^[27] **2**,^[28] **5**,^[5c] and **8**^[29] were prepared according to literature procedures. Thin-layer chromatography (TLC) was carried out on aluminum sheets coated with silica-gel 60 (Merck 5554). Column chromatography was performed on silica-gel 60 (Merck, 40–63 nm). Liquid secondary-ion mass spectra (LSIMS) were recorded on a VG ZabSpec mass spectrometer, equipped with a cesium ion source using *m*-nitrobenzyl alcohol, containing a trace amount of NaOAc. For high-resolution LSIMS (HRLSIMS), the instrument was operated at a resolution of about 6000 by employing narrow-range voltage scanning along with polyethylene glycol or CsI as reference compounds. Optical rotation measurements were measured at 23°C on a Perkin–Elmer 457 polarimeter. ^1H NMR Spectra were recorded on a Bruker AC300 (300 MHz), a Bruker AMX400 (400 MHz), or a Bruker ARX500 (500 MHz) spectrometer. ^{13}C NMR Spectra were recorded on either a Bruker AC300 (75.5 MHz) or on a Bruker AMX400 (100.6 MHz) spectrometer. The chemical shift values are expressed as δ values in ppm and the coupling constant values (J) are in Hertz.

Absorption spectra, circular dichroism spectra, and luminescence quenching experiments: Measurements were carried out at 22°C on air-equilibrated MeCN (Merck UvasolTM) or H_2O (milliQ, $18.2 \text{ M}\Omega\text{cm}$) solutions in the concentration range from 5×10^{-5} to $1 \times 10^{-3} \text{ mol L}^{-1}$. UV/Vis absorption and circular dichroism spectra were recorded with a Perkin–Elmer λ 16 spectrophotometer and a Jasco J-810 spectropolarimeter, respectively, and uncorrected luminescence spectra were obtained with a Perkin–Elmer LS-50 spectrofluorimeter equipped with a Hamamatsu R928 phototube. Luminescence lifetimes were measured by time-correlated single-photon counting with Edinburgh Instruments DS199 equipment (D_2 -filled arc lamp, $\lambda_{\text{ex}} = 300 \text{ nm}$). For the quenching studies, increasing amounts of the dendrimer were weighed and added to an air-equilibrated, dilute ($5 \times 10^{-5} \text{ mol L}^{-1}$) MeCN or H_2O solution of $[\text{Ru}(\text{bpy})_3](\text{ClO}_4)_2$. Tetrabutylammonium hexafluorophosphate (0.05 mol L^{-1}) or sodium perchlorate (0.05 mol L^{-1}) were employed as ionic strength buffers in MeCN and H_2O , respectively. For each solution, the luminescence intensity ($\lambda_{\text{ex}} = 450 \text{ nm}$, $\lambda_{\text{em}} = 610 \text{ nm}$) and lifetime were measured.

Electrochemical measurements: Cyclic voltammetric (CV) and differential pulse voltammetric (DPV) experiments were carried out in argon-purged

MeCN (Romil Hi-Dry) or H₂O (milliQ, 18.2 MΩ cm) solution at 22 °C with an Autolab 30 multipurpose instrument interfaced to a personal computer. The working electrode was a glassy carbon electrode (Amel); its surface was routinely polished with a 0.05 μm alumina-water slurry on a felt surface immediately prior to use. In all cases, the counter electrode was a Pt wire; in MeCN, a quasi-reference electrode (Ag wire) was employed and ferrocene was present as an internal standard, while in H₂O, a saturated calomel electrode (SCE) was used as the reference electrode. The concentrations of the compounds examined were 5.0×10^{-4} mol L⁻¹ for the protected species and 1.0×10^{-3} mol L⁻¹ for the deprotected ones; tetrabutylammonium hexafluorophosphate (0.05 mol L⁻¹) and sodium perchlorate (0.1 mol L⁻¹) were added as supporting electrolyte in MeCN and water, respectively. Cyclic voltammograms were obtained at sweep rates varying from 20 mV s⁻¹ to 10 V s⁻¹; DPV experiments were performed with a scan rate of 20 mV s⁻¹, a pulse height of 75 mV, and a duration of 40 ms. The iR compensation of the Autolab 30 was used, and efforts were made throughout the experiments in order to minimize the uncompensated resistance of the solution. The values of the diffusion coefficients of the dendrimers were obtained by chronocoulometry from the fitting of the Q versus $t^{1/2}$ plots (pulse width, 2 s; potential step from 0 to +0.8 V vs SCE). The effective area of the electrode (0.096 ± 0.004 cm²) was determined with the same method by using ferrocene ($D_0 = 2.4 \times 10^{-5}$ cm² s⁻¹ in MeCN)^[30] as the electroactive species.

The values of the heterogeneous electron-transfer rate constants (k_0 in Tables 4 and 5) were first estimated by using the Nicholson method;^[31] such values were then employed in the digital simulations of the cyclic voltammograms, obtained by using the program Antigona.^[32] From optimization of the fitting of the digital simulations to the experimental CV curves for the full range of scan rates employed, the values of k_0 and of the charge-transfer coefficient α were obtained. The fitting and deconvolution of the DPV profile shown in Figure 3 were obtained by employing the equations proposed by Parry and Osteryoung.^[33]

The voltammetric experiments upon addition of β -cyclodextrin (β -CD) were performed with scan rates of 50, 100, and 200 mV s⁻¹. The diffusion coefficient of the complex was determined from the ratio of the anodic peak current of the compound alone to its value in the presence of a large excess of β -CD, where most of the guest is bound by the host. The stability constant of the complex was obtained by fitting of digital simulations to the experimental CV curves taken at different values of β -CD concentrations.

Molecular modeling: The compounds **3**, **4**, **6**, **7**, and **9–12**, as well as the complexes β -CD · **4** and β -CD · **10**, were constructed within the input mode of Macromodel 5.0.^[34] The geometries were optimized by employing the Polak–Ribiere conjugate gradient (PRCG) algorithm^[35] in conjunction with the MM2* force field^[36] as implemented in Macromodel 5.0. The minimized geometries were subjected to an equilibration molecular dynamics run of 20 ps (simulated temperature = 500 K, time-step = 1.5 fs), followed by a molecular dynamics run of 200 ps (simulated temperature = 500 K, time-step = 1.5 fs) using the MM2* force field. In all cases, 200 randomly selected geometries were minimized with the PRCG algorithm and the MM2* force field. In all calculations, parameters reported previously in the literature^[8c] were employed for the cyclopentadienyl rings. For the iron atom, a new atom type was defined (charge = +1.23, van der Waals radius = 1.40 Å) within the atom types file of Macromodel 5.0. The distances between the iron atom and all the carbon atoms of the cyclopentadienyl rings were constrained at 2.03 Å (force constant = 9999 kJ mol⁻¹ Å⁻², half-width restraint = 0.0 Å).

General procedure for the preparation of 2-O-[2,3,4,6-tetra(O-benzoyl)- β -D-glucopyranosyl]ethylaminocarbonyl ferrocene (3**), 1,1'-bis[2-O-[2,3,4,6-tetra(O-benzoyl)- β -D-glucopyranosyl]ethylaminocarbonyl] ferrocene (**6**), tris[O-[2,3,4,6-tetra(O-acetyl)- β -D-glucopyranosyl]methyl]methylaminocarbonyl ferrocene (**9**), and 1,1'-bis[tris[O-[2,3,4,6-tetra(O-acetyl)- β -D-glucopyranosyl]methyl]methylaminocarbonyl] ferrocene (**11**):** A solution of **1** or **5** (0.2 mmol) in dry PhH (3 mL) was added to a stirred solution of **2** or **8** (0.4 mmol) and Et₃N (45 mg, 0.5 mmol) in dry PhH (5 mL) at room temperature and under an atmosphere of N₂. After 5 h (24 h when **2** and **5** were employed), the solvent was distilled off under reduced pressure. The residue was purified by column chromatography (SiO₂) with the eluants indicated for the individual compounds. The products were isolated as orange oils.

Data for 3: Yield 92%; PhMe/EtOAc (7.25:2.75–6:4); [α]_D = +18.1 (c = 1 in CHCl₃); ¹H NMR (CDCl₃): δ = 3.54–3.61 (m, 1H), 3.61–3.69 (m, 1H), 3.79–3.85 (m, 1H), 4.04–4.10 (m, 1H), 4.17 (s, 5H), 4.21–4.25 (m, 3H), 4.50 (brs, 1H), 4.55 (dd, J = 5.3, 12.2 Hz, 1H), 4.61 (brs, 1H), 4.70 (dd, J = 3.0, 12.2 Hz, 1H), 4.95 (d, J = 7.9 Hz, 1H), 5.62 (dd, J = 7.9, 9.8 Hz, 1H), 5.75 (pt, J = 9.8 Hz, 1H), 5.99 (pt, J = 9.8 Hz, 1H), 6.14 (t, J = 5.6 Hz, 1H), 7.30–8.08 (m, 20H); ¹³C NMR (CDCl₃): δ = 39.0, 62.8, 67.9, 68.1, 69.4, 69.4, 69.6, 70.2, 72.0, 72.4, 72.6, 75.6, 101.3, 125.2–137.8, 165.1, 165.1, 165.7, 166.0, 170.2; LSIMS: m/z : 851 [M]⁺; HRLSIMS: m/z calcd for [M]⁺ (C₄₇H₄₁FeNO₁₁): 851.2029; found: 851.2018.

Data for 6: Yield 54%; PhMe/EtOAc (1:1); [α]_D = +21.7 (c = 1 in CHCl₃); ¹H NMR (CDCl₃): δ = 3.58–3.70 (m, 4H), 3.88–3.93 (m, 2H), 4.11–4.17 (m, 2H), 4.20 (s, 4H), 4.22–4.28 (m, 2H), 4.44 (s, 4H), 4.55 (dd, J = 5.1, 12.2 Hz, 2H), 4.71 (dd, J = 2.9, 12.2 Hz, 2H), 5.62 (d, J = 7.9 Hz, 2H), 5.65 (dd, J = 7.9, 9.8 Hz, 2H), 5.78 (pt, J = 9.8 Hz, 2H), 6.01 (pt, J = 9.8 Hz, 2H), 6.83 (brs, 2H), 7.23–8.07 (m, 40H); ¹³C NMR (CDCl₃): δ = 39.3, 62.9, 68.9, 69.4, 70.2, 70.3, 71.2, 71.4, 71.9, 72.3, 72.8, 101.1, 125.2–137.7, 165.1, 165.7, 166.0, 170.0; LSIMS: m/z : 1518 [M +H]⁺; HRLSIMS: m/z calcd for [M]⁺ (C₈₄H₇₂FeN₂O₂₂): 1516.3926; found: 1516.3951.

Data for 9: Yield 91%; PhMe/EtOAc (1:2); [α]_D = –22.0 (c = 1 in CHCl₃); ¹H NMR (CDCl₃): δ = 1.97–2.03 (m, 36H), 3.61–3.71 (m, 3H), 3.78 (d, J = 10.1 Hz, 3H), 4.09 (dd, J = 2.2, 12.3 Hz, 3H), 4.21 (s, 5H), 4.23–4.32 (m, 8H), 4.47 (d, J = 7.9, 3H), 4.51 (brs, 1H), 4.68 (brs, 1H), 4.97 (dd, J = 7.9, 9.6 Hz, 3H), 5.04 (pt, J = 9.6 Hz, 3H), 5.17 (pt, J_1 = J_2 = 9.6 Hz, 3H), 5.89 (s, 1H); ¹³C NMR (CDCl₃): δ = 20.5, 20.7, 20.8, 21.4, 59.1, 61.6, 67.4, 68.1, 68.8, 70.0, 70.5, 70.6, 71.4, 71.9, 72.6, 75.6, 101.2, 169.2, 169.4, 170.1, 170.6, 171.8; LSIMS: m/z : 1323 [M]⁺; HRLSIMS: m/z calcd for [M]⁺ (C₅₇H₇₃FeNO₃₁): 1323.3516; found: 1323.3576.

Data for 11: Yield 87%; PhMe/EtOAc (1:9–0.5:9.5); [α]_D = –26.7 (c = 1 in CHCl₃); ¹H NMR (CDCl₃): δ = 2.02–2.11 (m, 72H), 3.74–3.79 (m, 6H), 3.81 (d, J = 10.3 Hz, 6H), 4.15 (dd, J = 2.0, 12.3 Hz, 6H), 4.35 (d, J = 10.3 Hz, 6H), 4.36 (dd, J = 4.5, 12.3 Hz, 6H), 4.40 (brs, 2H), 4.51 (brs, 2H), 4.55 (d, J = 7.9 Hz, 6H), 4.67 (brs, 2H), 4.71 (brs, 2H), 5.02 (dd, J = 7.9, 9.6 Hz, 6H), 5.10 (pt, J = 9.6 Hz, 6H), 5.24 (pt, J = 9.6 Hz, 6H), 6.19 (s, 2H); ¹³C NMR (CDCl₃): δ = 20.6, 59.4, 61.5, 68.1, 68.6, 69.7, 70.0, 71.3, 71.7, 72.5, 72.9, 73.0, 101.1, 169.1, 169.3, 169.9, 170.0, 170.4; LSIMS: m/z : 2462 [M +H]⁺; HRLSIMS: m/z calcd for [M]⁺ (C₁₀₄H₁₃₆FeN₆O₆₂): 2460.6900; found: 2460.6989.

General procedure for the preparation of 2-O-(β -D-glucopyranosyl)ethylaminocarbonyl ferrocene (4**), 1,1'-bis[2-O-(β -D-glucopyranosyl)ethylaminocarbonyl] ferrocene (**7**), tris[O-(β -D-glucopyranosyl)methyl]methylaminocarbonyl ferrocene (**10**), and 1,1'-bis[tris[O-(β -D-glucopyranosyl)methyl]methylaminocarbonyl] ferrocene (**12**):** A solution of NaOMe (14 mg, 0.3 mmol) in MeOH (0.3 mL) was added to a stirred solution of **3**, **6**, **9**, or **11** (0.3 mmol) in MeOH (10 mL) at room temperature under an atmosphere of N₂. After 6 h (3 h when **11** was employed), Amberlyst 15 (H⁺ form) was added, and the resulting mixture was filtered. The solvent was distilled off under reduced pressure, and the residue was dissolved in H₂O (50 mL) and washed with Et₂O (2 × 30 mL). The aqueous layer was concentrated under reduced pressure to afford the product quantitatively as an orange oil.

Data for 4: [α]_D = –6.1 (c = 1 in H₂O); ¹H NMR (D₂O): δ = 3.23 (dd, J = 7.9, 9.3 Hz, 1H), 3.28 (pt, J = 9.3 Hz, 1H), 3.34–3.38 (m, 1H), 3.41 (pt, J = 9.3 Hz, 1H), 3.42–3.46 (m, 1H), 3.49–3.55 (m, 1H), 3.62 (dd, J = 5.9, 12.0 Hz, 1H), 3.70–3.77 (m, 1H), 3.82 (dd, J = 3.1, 12.0 Hz, 1H), 3.93–4.00 (m, 1H), 4.21 (s, 5H), 4.41 (d, J = 7.9, 1H), 4.44 (brs, 2H), 4.72 (brs, 2H); ¹³C NMR (D₂O): δ = 39.2, 60.6, 68.1, 68.3, 68.4, 69.5, 69.9, 71.4, 73.0, 73.6, 75.5, 75.8, 102.2, 174.1; LSIMS: m/z : 436 [M +H]⁺; HRLSIMS: m/z calcd for [M +H]⁺ (C₁₉H₂₆FeNO₇): 436.1060; found: 436.1059.

Data for 7: [α]_D = –54.0 (c = 1 in H₂O); ¹H NMR (D₂O): δ = 3.16–3.29 (m, 4H), 3.32–3.42 (m, 4H), 3.48–3.55 (m, 2H), 3.56–3.64 (m, 2H), 3.70–3.76 (m, 2H), 3.77–3.84 (m, 2H), 3.86–3.96 (m, 2H), 4.34–4.39 (m, 2H), 4.41 (d, J = 8.0 Hz, 2H), 4.45 (brs, 2H), 4.66 (brs, 2H), 4.81 (brs, 2H), 4.87 (brs, 2H); ¹³C NMR (D₂O): δ = 39.2, 60.5, 68.2, 69.4, 69.6, 69.7, 72.8, 73.0, 75.4, 75.6, 102.1, 172.5; LSIMS: m/z : 685 [M +H]⁺; HRLSIMS: m/z calcd for [M +H]⁺ (C₂₈H₄₁FeN₂O₁₄): 685.1907; found: 985.1885.

Data for 10: [α]_D = –45.3 (c = 1 in H₂O); ¹H NMR (D₂O): δ = 3.13 (dd, J = 9.4, 7.9 Hz, 3H), 3.16 (pt, J = 9.4 Hz, 3H), 3.23–3.27 (m, 3H), 3.30 (pt, J = 9.4 Hz, 3H), 3.52 (dd, J = 6.0, 12.3 Hz, 3H), 3.71 (dd, J_1 = 2.0 Hz, J_2 = 12.3 Hz, 3H), 3.82 (d, J = 10.5 Hz, 3H), 4.15 (s, 5H), 4.21 (d, J = 10.5 Hz, 3H), 4.31 (d, J = 7.9 Hz, 3H), 4.34 (brs, 2H), 4.63 (brs, 2H); ¹³C NMR

(D₂O): δ = 59.7, 60.6, 67.4, 69.3, 69.6, 71.2, 72.1, 72.9, 75.4, 75.7, 102.7, 174.1; LSIMS: m/z : 820 [M+H]⁺; HRLSIMS: m/z calcd for [M+H]⁺ (C₃₃H₅₀FeNO₁₉): 820.2326; found: 820.2365.

Data for 12: [α]_D = −59.6 (c = 1 in H₂O); ¹H NMR (D₂O): δ = 3.22 (dd, J = 9.3, 7.9 Hz, 6H), 3.26 (pt, J = 9.3 Hz, 6H), 3.31–3.37 (m, 6H), 3.39 (pt, J = 9.3 Hz, 6H), 3.60 (dd, J = 5.2, 12.2 Hz, 6H), 3.80 (dd, J = 2.0, 12.2 Hz, 6H), 3.91 (d, J = 10.1 Hz, 6H), 4.29 (d, J = 10.1 Hz, 6H), 4.40 (d, J = 7.9 Hz, 6H), 4.50 (brs, 4H), 4.80 (brs, 4H); ¹³C NMR (D₂O): δ = 59.6, 60.6, 67.4, 69.5, 69.9, 72.9, 74.3, 75.4, 75.7, 102.7, 174.1; LSIMS: m/z : 1453 [M+H]⁺.

Complexes β -CD·4 and β -CD·10: The complex β -CD·4 or β -CD·10 was prepared by mixing β -CD and 4 or 10, respectively, in D₂O at ambient temperature. β -CD·4: LSIMS: m/z : 1570 [M]⁺. β -CD·10: LSIMS: m/z : 1954 [M]⁺.

Acknowledgement

This research was supported by the European Community (Marie Curie fellowship to M.C.-L. and contract HPRN-CT-2000–00029), MURST (Supramolecular Devices Project), and the University of Bologna (Young Researchers grant to A.C.). We thank the FRAE-CNR Institute, Bologna, for allowing us to use the spectropolarimeter.

- [1] For accounts and reviews on ferrocene-based molecular and supramolecular systems, see: a) E. C. Constable, *Angew. Chem.* **1991**, *103*, 418–419; *Angew. Chem. Int. Ed. Engl.* **1991**, *30*, 407–408; b) G. W. Gokel, J. C. Medina, C. Li, *Synlett* **1991**, 677–683; c) P. D. Beer, *Adv. Inorg. Chem.* **1992**, *39*, 79–157; d) R. Isnin, A. E. Kaifer, *Pure Appl. Chem.* **1993**, *65*, 495–498; e) P. D. Beer, *Adv. Mater.* **1994**, *6*, 607–609; f) P. D. Beer, *Chem. Commun.* **1996**, 689–696; g) F. M. Raymo, J. F. Stoddart, *Chem. Ber.* **1996**, *129*, 981–990; h) F. M. Raymo, J. F. Stoddart, *Pure Appl. Chem.* **1996**, *68*, 313–322; i) P. D. Beer, *Acc. Chem. Res.* **1998**, *31*, 71–80; j) P. D. Beer, P. A. Gale, G. Z. Chen, *Coord. Chem. Rev.* **1999**, *186*, 3–36.
- [2] For accounts and reviews on molecular and supramolecular devices, which can be controlled by external stimuli, see: a) A. P. de Silva, H. Q. N. Gunaratne, T. Gunnlaugsson, A. J. M. Huxley, C. P. McCoy, J. T. Rademacher, T. E. Rice, *Chem. Rev.* **1997**, *97*, 1515–1566; b) M. D. Ward, *Chem. Ind.* **1997**, 640–645; c) V. Balzani, M. Gómez-López, J. F. Stoddart, *Acc. Chem. Res.* **1998**, *31*, 405–414; d) P. L. Bouslas, M. Gómez-Kaifer, L. Echegoyen, *Angew. Chem.* **1998**, *110*, 226–258; *Angew. Chem. Int. Ed.* **1998**, *37*, 216–247; e) J.-P. Sauvage, *Acc. Chem. Res.* **1998**, *31*, 611–619; f) J.-C. Chambron, J.-P. Sauvage, *Chem. Eur. J.* **1998**, *4*, 1362–1366; g) A. Niemz, V. M. Rotello, *Acc. Chem. Res.* **1999**, *32*, 42–52; h) M. R. Bryce, *Adv. Mater.* **1999**, *11*, 11–23; i) A. E. Kaifer, *Acc. Chem. Res.* **1999**, *32*, 62–71; j) V. Balzani, A. Credi, M. Venturi in *Supramolecular Science: Where It Is and Where It Is Going* (Eds.: R. Ungaro, E. Dalcanele), Kluwer Academic, Dordrecht, **1999**, pp. 1–22; k) L. Fabbri, M. Licchelli, P. Pallavicini, *Acc. Chem. Res.* **1999**, *32*, 846–853; l) P. Piotrowski, *Chem. Soc. Rev.* **1999**, *28*, 143–150; m) D. A. Leigh, A. Murphy, *Chem. Ind.* **1999**, 178–183; n) V. Balzani, A. Credi, F. M. Raymo, J. F. Stoddart, *Angew. Chem.* **2000**, *112*, 3438–3530; *Angew. Chem. Int. Ed.* **2000**, *39*, 3348–3391; o) *Acc. Chem. Res.* **2001**, *34*, No. 6 (Special Issue on Molecular Machines).
- [3] a) P. R. Ashton, S. E. Boyd, C. L. Brown, N. Jayaraman, S. A. Nepogodiev, J. F. Stoddart, *Chem. Eur. J.* **1996**, *2*, 1115–1128; b) P. R. Ashton, S. E. Boyd, C. L. Brown, N. Jayaraman, J. F. Stoddart, *Angew. Chem.* **1997**, *109*, 756–759; *Angew. Chem. Int. Ed. Engl.* **1997**, *36*, 732–735; c) P. R. Ashton, S. E. Boyd, C. L. Brown, S. A. Nepogodiev, E. W. Meijer, H. W. I. Peerlings, J. F. Stoddart, *Chem. Eur. J.* **1997**, *3*, 974–984; d) N. Jayaraman, S. A. Nepogodiev, J. F. Stoddart, *Chem. Eur. J.* **1997**, *3*, 1193–1199; e) H. W. I. Peerlings, S. A. Nepogodiev, J. F. Stoddart, E. W. Meijer, *Eur. J. Org. Chem.* **1998**, 1879–1886; f) B. Colonna, V. D. Harding, S. A. Nepogodiev, F. M. Raymo, N. Spencer, J. F. Stoddart, *Chem. Eur. J.* **1998**, *4*, 1244–1254; g) P. R. Ashton, E. F. Hounsell, N. Jayaraman, T. M. Nilsen, N. Spencer, J. F. Stoddart, M. Young, *J. Org. Chem.* **1998**, *63*, 3429–3437; h) F. Cardullo, F. Diederich, L. Echegoyen, T. Habicher, N. Jayaraman, R. M. Leblanc, J. F. Stoddart, S. P. Wang, *Langmuir* **1998**, *14*, 1955–1959; i) G. M. Pavlov, E. V. Korneeva, K. Jumel, S. E. Harding, E. W. Meijer, H. W. I. Peerlings, J. F. Stoddart, S. A. Nepogodiev, *Carbohydr. Polym.* **1999**, *38*, 195–202.
- [4] For accounts and reviews on dendrimers, see: a) D. A. Tomalia, A. M. Naylor, W. A. Goddard III, *Angew. Chem.* **1990**, *102*, 119–157; *Angew. Chem. Int. Ed. Engl.* **1990**, *29*, 113–151; b) D. A. Tomalia, H. D. Durst, *Top. Curr. Chem.* **1993**, *165*, 193–313; c) J. Issberner, R. Moors, F. Vögtle, *Angew. Chem.* **1994**, *106*, 2507–2514; *Angew. Chem. Int. Ed. Engl.* **1994**, *33*, 2413–2420; d) R. F. Service, *Science* **1995**, *267*, 458–459; e) G. R. Newkome, C. N. Moorefield, F. Vögtle, *Dendritic Macromolecules*, VCH, Weinheim, **1996**; f) J. M. J. Fréchet, C. J. Hawker, *Compr. Polym. Sci. 2nd Suppl.* **1996**, 140–201; g) F. Zeng, S. C. Zimmerman, *Chem. Rev.* **1997**, *97*, 1681–1712; h) V. Balzani, S. Campagna, G. Denti, A. Juris, S. Serroni, M. Venturi, *Acc. Chem. Res.* **1998**, *31*, 26–34; i) H. Frey, C. Lach, K. Lorenz, *Adv. Mater.* **1998**, *10*, 279–293; j) C. Gorman, *Adv. Mater.* **1998**, *10*, 295–309; k) M. R. Bryce, W. Devonport, L. M. Goldenberg, C. Wang, *Chem. Commun.* **1998**, 945–951; l) R. J. Puddephatt, *Chem. Commun.* **1998**, 1055–1062; m) D. K. Smith, F. Diederich, *Chem. Eur. J.* **1998**, *4*, 1353–1361; n) A. Archut, F. Vögtle, *Chem. Soc. Rev.* **1998**, *27*, 233–240; o) O. A. Matthews, A. N. Shipway, J. F. Stoddart, *Prog. Polym. Sci.* **1998**, *23*, 1–56; p) E. F. Vögtle, *Top. Curr. Chem.* **1998**, *197*, 1–228; q) M. Fischer, F. Vögtle, *Angew. Chem.* **1999**, *111*, 934–955; *Angew. Chem. Int. Ed.* **1999**, *38*, 885–905; r) A. W. Bosman, H. M. Janssen, E. W. Meijer, *Chem. Rev.* **1999**, *99*, 1665–1688; s) G. R. Newkome, E. F. He, C. N. Moorefield, *Chem. Rev.* **1999**, *99*, 1689–1746; t) J. P. Majoral, A. M. Caminade, *Chem. Rev.* **1999**, *99*, 845–880; u) U. Scherf, *Top. Curr. Chem.* **1999**, *201*, 163–222; v) A. Adronov, J. M. J. Fréchet, *Chem. Commun.* **2000**, 1701–1710; w) S. Hecht, J. M. J. Fréchet, *Angew. Chem.* **2001**, *113*, 76–94; *Angew. Chem. Int. Ed.* **2001**, *40*, 74–91; x) A. Juris, M. Venturi, P. Ceroni, V. Balzani, S. Campagna, S. Serroni, *Collect. Czech. Chem. Commun.* **2001**, *66*, 1–32; y) V. Balzani, P. Ceroni, A. Juris, M. Venturi, S. Campagna, F. Puntoriero, S. Serroni, *Coord. Chem. Rev.* **2001**, *219*–221, 585–613; z) D. C. Tully, J. M. J. Fréchet, *Chem. Commun.* **2001**, 1229–1239.
- [5] For examples of ferrocene-containing dendrimers, see: a) B. Alonso, I. Cuadrado, M. Morán, J. Losada, *J. Chem. Soc. Chem. Commun.* **1994**, 2575–2576; b) B. Alonso, M. Morán, C. M. Casado, F. Lobete, J. Losada, I. Cuadrado, *Chem. Mater.* **1995**, *7*, 1440–1442; c) I. Cuadrado, M. Morán, C. M. Casado, B. Alonso, F. Lobete, B. García, M. Ibasate, J. Losada, *Organometallics* **1996**, *15*, 5278–5280; d) C. Valerio, J. L. Fillaut, J. Ruiz, J. Guittard, J. C. Blais, D. Astruc, *J. Am. Chem. Soc.* **1997**, *119*, 2588–2589; e) S. Rigaut, M. H. Delville, D. Astruc, *J. Am. Chem. Soc.* **1997**, *119*, 1132–1133; f) R. Castro, I. Cuadrado, B. Alonso, C. M. Casado, M. Morán, A. E. Kaifer, *J. Am. Chem. Soc.* **1997**, *119*, 5760–5761; g) C. M. Cardona, A. E. Kaifer, *J. Am. Chem. Soc.* **1998**, *120*, 4023–4024; h) C. M. Casado, I. Cuadrado, M. Morán, B. Alonso, B. García, B. Gonzalez, J. Losada, *Coord. Chem. Rev.* **1999**, *186*, 53–79; i) D. K. Smith, *J. Chem. Soc. Perkin Trans. 2* **1999**, 1563–1565; j) Y. Wang, C. M. Cardona, A. E. Kaifer, *J. Am. Chem. Soc.* **1999**, *121*, 9756–9757; k) C. M. Casado, B. Gonzáles, I. Cuadrado, B. Alonso, M. Morán, J. Losada, *Angew. Chem.* **2000**, *112*, 2219–2222; *Angew. Chem. Int. Ed.* **2000**, *39*, 2135–2138; l) S. Nlate, J. Ruiz, V. Sartor, R. Navarro, J.-C. Blais, D. Astruc, *Chem. Eur. J.* **2000**, *6*, 2544–2553; m) C. M. Cardona, T. Donovan McCarley, A. E. Kaifer, *J. Org. Chem.* **2000**, *65*, 1857–1864; n) J. Alvarez, T. Ren, A. E. Kaifer, *Organometallics* **2001**, *20*, 3543–3549.
- [6] For recent examples of dendrimers bearing an electroactive core, see refs. [5g,i] and: a) F. Vögtle, M. Plevovets, M. Nieger, G. C. Azzellini, A. Credi, L. De Cola, V. De Marchis, M. Venturi, V. Balzani, *J. Am. Chem. Soc.* **1999**, *121*, 6290–6298; b) M. Kimura, Y. Sugihara, T. Muto, K. Hanabusa, H. Shirai, N. Kobayashi, *Chem. Eur. J.* **1999**, *5*, 3495–3500; c) P. Weiermann, J.-P. Gisselbrecht, C. Boudon, F. Diederich, M. Gross, *Angew. Chem.* **1999**, *38*, 3400–3404; *Angew. Chem. Int. Ed.* **1999**, *38*, 3215–3219; d) C. B. Gorman, J. C. Smith, M. W. Hager, B. L. Parkhurst, H. Sierzputowska-Gracz, C. A. Haney, *J. Am. Chem. Soc.* **1999**, *121*, 9958–9966; e) M. Kimura, T. Shiba, T. Muto, K. Hanabusa, H. Shirai, *Chem. Commun.* **2000**, 11–12; f) R. Toba, J. M. Quintela, C. Peinador, E. Román, A. E. Kaifer, *Chem. Commun.* **2001**, 857–858; g) P. Ceroni, V. Vicinelli, M. Maestri, V. Balzani, W. M. Müller, U. Müller, U. Hahn, F. Osswald, F. Vögtle, *New J. Chem.* **2001**, *25*, 989–993.

- [7] A. L. Lenninger, D. L. Nelson, M. M. Cox, *Principles of Biochemistry*, Worth, New York, **1994**.
- [8] For examples of complexes formed between ferrocene derivatives and cyclodextrins, see: a) B. Siegel, R. Breslow, *J. Am. Chem. Soc.* **1975**, *97*, 6869–6870; b) R. Breslow, M. F. Czarniecki, J. Emert, H. Hamaguchi, *J. Am. Chem. Soc.* **1980**, *102*, 762–770; c) H.-J. Thiem, M. Brandl, R. Breslow, *J. Am. Chem. Soc.* **1988**, *110*, 8612–8616; d) A. Harada, S. Takahashi, *J. Chem. Soc. Chem. Commun.* **1984**, 645–646; e) A. Harada, S. Takahashi, *J. Inclusion Phenom.* **1984**, *2*, 791–798; f) T. Matsue, T. Osa, D. H. Evans, *J. Inclusion Phenom.* **1984**, *2*, 547–554; g) T. Matsue, D. H. Evans, T. Osa, N. Kobayashi, *J. Am. Chem. Soc.* **1985**, *107*, 3411–3417; h) A. Ueno, F. Moriawaki, T. Osa, F. Hamada, K. Murai, *Tetrahedron Lett.* **1985**, *26*, 899–902; i) T. Matsue, T. Kato, U. Akiba, T. Osa, *Chem. Lett.* **1986**, 843–846; j) T. Osa, N. Kobayashi, *Chem. Lett.* **1986**, 421–424; k) A. Ueno, I. Suzuki, T. Osa, *Makromol. Chem. Rapid Commun.* **1987**, *8*, 131–134; l) F. M. Menger, M. J. Sherrod, *J. Am. Chem. Soc.* **1988**, *110*, 8606–8611; m) R. Isnin, C. Salam, A. E. Kaifer, *J. Org. Chem.* **1991**, *56*, 35–41; n) L. A. Godínez, S. Patel, C. M. Criss, A. E. Kaifer, *J. Phys. Chem.* **1995**, *99*, 17449–17455; o) R. M. Nielson, L. A. Lyon, J. T. Hupp, *Inorg. Chem.* **1996**, *35*, 970–973; p) Y. M. Li, X. J. Yao, X. Feng, X. M. Wang, J. T. Wang, *J. Organomet. Chem.* **1996**, *509*, 221–224; q) J. S. Wu, K. Toda, A. Tanaka, I. Sanemasa, *Bull. Chem. Soc. Jpn.* **1998**, 1615–1618; r) R. C. Sabapathy, S. Bhattacharyya, W. E. Cleland, C. L. Hussey, *Langmuir* **1998**, *14*, 3797–3807; s) H. X. Ju, D. Leech, *Langmuir* **1998**, *14*, 300–306; t) A. E. Kaifer, *Acc. Chem. Res.* **1999**, *32*, 62–71; u) J. Liu, R. Castro, K. A. Abboud, A. E. Kaifer, *J. Org. Chem.* **2000**, *65*, 6973–6977.
- [9] A. B. P. Lever, *Inorganic Electronic Spectroscopy*, Elsevier, Amsterdam, **1984**.
- [10] S. Fery-Forgues, B. Delavaux-Nicot, *J. Photochem. Photobiol. A* **2000**, *132*, 137–159.
- [11] At 293 K: water, 1.00 mPa s; acetonitrile, 0.34 mPa s (*CRC Handbook of Chemistry and Physics*, 75th ed. (Ed.: D. R. Lide), CRC, Boca Raton, **1994**). According to the Stokes–Einstein equation, the diffusion coefficient is linearly related to $1/\eta$, where η is the viscosity of the solvent.
- [12] H. I. Kim, J. E. Houston, *J. Am. Chem. Soc.* **2000**, *122*, 12045–12046.
- [13] The global minima for **7** and **12** that are shown in Figure 2 were found by molecular dynamics/multiconformer minimizations performed in the “gas phase”. Under these conditions, intramolecular hydrogen-bonding interactions between the amide groups and between the deprotected β -D-glucopyranosyl residues favor *cisoid* conformations. The electrochemical measurements were performed, instead, in water. Not surprisingly, this highly polar media has a depressive effect on the intramolecular hydrogen-bonding interactions and favors *transoid* conformations.
- [14] A. Juris, V. Balzani, F. Barigelli, S. Campagna, P. Belser, A. von Zelewsky, *Coord. Chem. Rev.* **1988**, *84*, 85–277.
- [15] V. Balzani, L. Moggi, M. F. Manfrin, F. Bolletta, G. S. Laurence, *Coord. Chem. Rev.* **1975**, *15*, 321–433.
- [16] S. L. Murov, I. Carmichael, G. L. Hug, *Handbook of Photochemistry*, 2nd ed., Marcel Dekker, New York, **1993**.
- [17] M. Z. Hoffmann, F. Bolletta, L. Moggi, G. L. Hug, *J. Phys. Chem. Ref. Data* **1989**, *18*, 219–543.
- [18] F. Scandola, V. Balzani, *J. Chem. Educ.* **1983**, *60*, 814–823.
- [19] E. J. Lee, M. S. Wrighton, *J. Am. Chem. Soc.* **1991**, *113*, 8562–8564.
- [20] Th. Förster, *Discuss. Faraday Soc.* **1959**, *27*, 7–17.
- [21] D. L. Dexter, *J. Chem. Phys.* **1953**, *21*, 836–850.
- [22] S. Encinas, N. R. M. Simpson, P. Andrews, M. D. Ward, C. M. White, N. Armaroli, F. Barigelli, A. Houlton, *New J. Chem.* **2000**, *24*, 987–991.
- [23] P. Piotrowski in *Electron Transfer in Chemistry*, Vol. 1 (Ed.: V. Balzani), Wiley-VCH, Weinheim, **2001**, pp. 215–237.
- [24] For similar findings, see ref. [5c].
- [25] a) *Comprehensive Supramolecular Chemistry*, Vol. 3: Cyclodextrins (Eds.: J. Szejtli, T. Osa), Pergamon, Oxford, **1996**; b) G. Marconi, B. Mayer, *Pure Appl. Chem.* **1997**, *69*, 779–783.
- [26] D. D. Perrin, W. F. L. Armarego, *Purification of Laboratory Chemicals*, 3rd ed., Pergamon Press, Oxford, **1989**.
- [27] H.-J. Lorkowski, R. Pannier, A. Wende, *J. Prakt. Chem.* **1967**, *35*, 149–158.
- [28] P. R. Ashton, S. R. L. Everitt, M. Gómez-López, N. Jayaraman, J. F. Stoddart, *Tetrahedron Lett.* **1997**, *38*, 5691–5694.
- [29] P. R. Ashton, S. E. Boyd, C. L. Brown, N. Jayaraman, S. A. Nepogodiev, J. F. Stoddart, *Chem. Eur. J.* **1996**, *2*, 1115–1128.
- [30] T. Kuwana, D. E. Bublitz, G. Hoh, *J. Am. Chem. Soc.* **1960**, *82*, 5811–5817.
- [31] R. S. Nicholson, *Anal. Chem.* **1965**, *37*, 1351–1354.
- [32] Antigona was developed by Dr. Loic Möttier and can be downloaded from: <http://www.ciam.unibo.it/electrochem.html/Research/research.html>.
- [33] E. P. Parry, R. A. Osteryoung, *Anal. Chem.* **1965**, *37*, 1634–1637.
- [34] F. Mohamadi, N. G. J. Richards, W. C. Guida, R. Liskamp, M. Lipton, C. Caufield, G. Chang, T. Hendrickson, W. C. Still, *J. Comput. Chem.* **1990**, *11*, 440–467.
- [35] E. Polak, G. Ribiere, *Rev. Fr. Inf. Rech. Oper.* **1969**, *16-R1*, 35–43.
- [36] N. L. Allinger, *J. Am. Chem. Soc.* **1977**, *99*, 8127–8134.

Received: June 11, 2001 [F3328]